TISSUE ENGINEERING: Part A
Volume 20, Numbers 3 and 4, 2014

DOI: 10.1089/ten.tea.2013.0205

Proteomic Analysis Profile of Engineered Articular Cartilage with Chondrogenic Differentiated Adipose Tissue-Derived Stem Cells Loaded Polyglycolic Acid Mesh for Weight-Bearing Area Defect Repair

Lunli Gong, PhD, MD,[1,*] Xiao Zhou, PhD, MD,[2,*] Yaohao Wu, MD,[1] Yun Zhang, PhD, MD,[1] Chen Wang, PhD, MD,[1] Heng Zhou, PhD,[1] Fangfang Guo, PhD, MD,[1] and Lei Cui, PhD, MD[1,3]

The present study was designed to investigate the possibility of full-thickness defects repair in porcine articular cartilage (AC) weight-bearing area using chondrogenic differentiated autologous adipose-derived stem cells (ASCs) with a follow-up of 3 and 6 months, which is successive to our previous study on nonweight-bearing area. The isolated ASCs were seeded onto the phosphoglycerate/polylactic acid (PGA/PLA) with chondrogenic induction *in vitro* for 2 weeks as the experimental group prior to implantation in porcine AC defects (8 mm in diameter, deep to subchondral bone), with PGA/PLA only as control. With follow-up time being 3 and 6 months, both neo-cartilages of postimplantation integrated well with the neighboring normal cartilage and subchondral bone histologically in experimental group, whereas only fibrous tissue in control group. Immunohistochemical and toluidine blue staining confirmed similar distribution of COL II and glycosaminoglycan in the regenerated cartilage to the native one. A vivid remolding process with repair time was also witnessed in the neo-cartilage as the compressive modulus significantly increased from 70% of the normal cartilage at 3 months to nearly 90% at 6 months, which is similar to our former research. Nevertheless, differences of the regenerated cartilages still could be detected from the native one. Meanwhile, the exact mechanism involved in chondrogenic differentiation from ASCs seeded on PGA/PLA is still unknown. Therefore, proteome is resorted leading to 43 proteins differentially identified from 20 chosen two-dimensional spots, which do help us further our research on some committed factors. In conclusion, the comparison via proteome provided a thorough understanding of mechanisms implicating ASC differentiation toward chondrocytes, which is further substantiated by the present study as a perfect supplement to the former one in nonweight-bearing area.

Introduction

Articular cartilage (AC) forms a specialized, smooth connective tissue for weight bearing and serves as a smooth gliding surface allowing movement of the joints as well as shock absorption. The prevalence of disorders suffered from trauma and aging affecting AC is increasing owing to its low self-regeneration ability. Eventually, AC damage results in osteoarthritis, which is characterized by irreversible degeneration and dysfunction.[1–3] Repair of defects in AC remains a challenge for the unsatisfactory effects of the current clinical practice. The emerging of tissue engineering base on seed cell and biomaterial scaffold provided an alternative approach to correct pathological injuries or to restore defects in AC. Among the identified adult mesenchymal stem cells (MSCs), adipose derived stem cells (ASCs) has drawn more attention in tissue engineering application for its abundant source, easier accessibility, and phenotype stability in addition to its multipotential differentiation toward osteogenic, chondrogenic, adipogenic, myogenic, neurogenic, and angiogenic lineages.[4–8] In a previous study, using ASCs seeded within fibrous phosphoglycerate (PGA) mesh, we have successfully repaired full thickness AC defects in nonweight-bearing area in a porcine model.

[1]Department of Plastic and Reconstructive Surgery, Shanghai 9th People's Hospital, Shanghai Jiao Tong University School of Medicine, Shanghai, People's Republic of China.
[2]Department of Tumor Plastic Surgery of Tumor Hospital, Xiangya School of Medicine of Central South University, Changsha, People's Republic of China.
[3]Institute of Biomedical Engineering, Medical Technology and Engineering of Henan University of Science and Technology, Luoyang, People's Republic of China.
*These authors equally contributed to this work.

However, as PGA mesh showed limited biomechanical strength, whether chondrogenesis-induced ASCs combined with PGA scaffold could heal defects in weight-bearing area in a porcine model, which exhibits size and cartilage thickness similar to that of humans, remains to be explored.

Up to now, with the rapid development of tissue engineering, accumulating evidence reported have documented that AC could be regenerated with MSC-based engineered cartilage. However, all these data also suggest that differences are still present between the engineered and native cartilage. The defect was repaired actually in a "similar" rather than the "same" way as compared with normal cartilage in cellular orientation, extracellular matrix (ECM) content and alignment, biomechanical properties. Therefore, to better understand the mechanisms implicated in the formation of engineered cartilage *in vivo*, exploring some novel means is important for discriminating the engineered cartilage from normal ones at the whole tissue level. Tissue-based proteome has been documented to decipher the proteome complexities of tissue microenvironment and thereby to deliver important information with appropriate pathologic and histological relevance.[9–13] By proteome analysis, normal human AC proteome was established by Ruiz-Romero C that annexins, vimentin, transgelin, destrin, cathepsin D, heat shock protein 47, and mitochondrial superoxide dismutase were more abundant in chondrocytes.[14] One extensive prefractionation technique followed by two-dimensional (2D) E gel separation was first proposed by Vincourt[15] *et al.*, which could set us one positive control in tissue-engineered cartilage research.

Thus, the current research is designed to repair full thickness AC defects in weight-bearing area in a porcine model, using chondrogenic differentiated autologous ASCs seeded on PGA/polylactic acid (PLA) scaffold. In addition, proteome is resorted to exploring the potential mechanisms involved in cartilage regeneration at whole profile of protein level. We expected that these results could provide us some mechanical cues to remove the discernible difference between native and engineered cartilage.

Materials and Methods

Isolation and culture of adult ASCs

The experimental protocol was approved by the Animal Care and Experiment Committee of Shanghai Jiao Tong University School of Medicine. Autologous subcutaneous adipose tissue in the nape was yielded from 1-year-old pigs (Chang Feng hybrid pigs), ignoring animal genders (male 11 while female 5), after anesthetization through intramuscular injection of ketamine (10 mg/kg). ASCs were isolated from the adipose tissue as mentioned by Valina *et al.*[16] Briefly, adipose tissue was washed thrice with 0.1 M phosphate-buffered saline (PBS, pH 7.4) and treated with 0.075% type I collagenase (Washington Biochemical Corp.) at 37°C for 30 min. Enzymatic activity was neutralized with low glucose Dulbecco's Modified Eagle's Medium (LG-DMEM; Gibco) with 10% fetal bovine serum (FBS; HyClone) prior to centrifugation at 1200 g for 10 min. The cells obtained were resuspended in LG-DMEM culture medium containing 10% FBS, 100 mg/mL streptomycin and 100 U/mL penicillin (defined as the growth medium), and plated at 4×10^4 cells/cm^2 in Φ 100 mm culture dishes (Falcon) with the medium changed every 3 days. Cells were passaged with 70–80% confluence and ASCs prior to passage 3 were used in the following study.

Preparation of PGA/PLA scaffold and cell seeding

Following previous report,[17] 30 mg of unwoven PGA fibers (Shanghai Ju Rui Biomaterials Company, Inc.) with diameters being 20–30 mm were pressed into a silicone rubber mold with diameter of 8 mm while thickness 6 mm. The shape of PGA scaffold in mold was stabilized by 0.3 mL polylactic acid (PLA; Sigma–Aldrich) solution (1.5% in dichloromethane) via instillation, which was then kept in fume hood for 10 min for solvent evaporation. Thereafter, the PGA/PLA complexes were removed from the mold and sterilized in 75% alcohol for 1 h prior to PBS wash thrice and finally, soaked overnight in the growth medium. The excessive medium left in scaffolds was thoroughly aspirated before they were air-dried for 30 min under ultraviolet light.

ASCs harvested were resuspended in the culture medium at a density of 5.0×10^7 cells/mL. Aliquots of 0.3 mL cell suspensions were then evenly seeded by instillation into PGA/PLA scaffolds followed by 3 h incubation for cell attachment before addition of either 6 mL of the growth medium or chondrogenesis-inducing medium (the growth medium further supplemented with 10 ng/mL transforming growth factor-β1 [TGF-β1], 100 ng/mL insulin-like growth factor-1 [IGF-1], 40 ng/mL dexamethasone, and 6.25 mg/mL transferrin [all from Sigma–Aldrich]). The cell–PGA constructs in both media were subsequently cultured *in vitro* for 2 weeks respectively, with the media changed twice a week, before implantation in porcine defects to be described later.

Surgical procedures

As described previously,[17] an AC defect deep into subchondral bone 8 mm in diameter and 6 mm in depth was created by drilling using a trephine at porcine weight-bearing area of femur trochlea in one randomly chosen knee. While the same procedure was performed at the contralateral knee joint with two defects created in each pig. After removal of blood clots, the defect randomly chosen was repaired with the autologous chondrogenic cell–PGA/PLA construct as the experimental group, while the other with PGA/PLA scaffold alone as the control group. Finally, the implant was stabilized by a crossing transosseous fixation using biodegradable sutures to ensure a good integration of the implant with its surrounding native tissue.[18] Postoperatively, all animals ($n=16$) were allowed to move without limitation. After 3 and 6 months, animals were euthanized for sample harvest, respectively.

Macrographic examination and grading

The harvested samples including the cartilage defect and the underlying cancellous bone were examined grossly before slicing through the middle line of the defects to see its longitudinal cross section and the interface between the repaired and the adjacent normal tissue. The repair was graded grossly according to the criteria reported and previously listed in Table 1.[19] Then, some samples were used for histological examination and immunohistochemical (IHC) staining, while others were for biomechanical assay,

Table 1. Grading Scale for Gross Appearance

Description	*Points*
Intraarticular adhesions	
None	2
Minimal/fine loose fibrous tissue	1
Major/dense fibrous tissue	0
Restoration of articular surface	
Complete restoration	2
Partial restoration	1
No restoration	0
Erosion of cartilage	
None	2
Defect site/site border	1
Defect site and adjacent normal cartilage	0
Appearance of cartilage	
Translucent	2
Opaque	1
Discolored or irregular	0
Maximum total	8

This table was cited from Cook *et al.*'s[19] grading scale without modification.

glycosaminoglycans (GAG) content determination, and proteome analysis.

Histological examination and grading

The samples obtained were fixed, decalcified, and embedded in paraffin to be sectioned in 5 mm slices. The slices were then stained with hematoxylin and eosin (H&E) and toluidine blue, respectively. According to the scoring system described by Wakitani *et al.*,[20] the histological grading was carried out as a blind test by three independent individuals in accordance with the histological structure, matrix staining, surface regularity, thickness of the repaired cartilage, and integration of the repaired tissue with its surrounding normal one as shown in Table 2.

IHC staining

Expression of collagen type II (COL II) in the engineered cartilage was examined by IHC staining at 3 and 6 months postsurgery, respectively. Briefly, paraffin sections were deparaffinized followed by hydration in gradient ethanol solutions (100% to 70%). Then, endogenous peroxidase activity was inactivated with 3% hydrogen peroxide incubation for 15 min at room temperature. Nonspecific binding was blocked by 10% normal goat serum diluted in 0.1 M PBS at 37°C for 30 min. The section was then incubated at 37°C for 1 h with mouse anti-collagen-II monoclonal antibody (Santa Cruz) diluted in 0.1M PBS (1:200), followed by incubation with 1:100 diluted horseradish peroxidase (HRP)-conjugated anti-mouse antibody (DAKO) for 30 min at 37°C. Finally, color was developed with diaminobenzidine tetrahydrochloride (DAB).

Biomechanical and biochemical analysis of the engineered cartilage

The biomechanical property of the engineered cartilage was tested by measuring the compressive modulus following previous description.[17] Briefly, the samples were trimmed to fit in a test chamber (5 mm in diameter) of the biomechanical analyzer (Instron5542). The force–displacement curve was obtained by employing a constant compressive strain at a rate of 1 mm/min until the maximal force at 450 N. The compressive modulus of the tested tissue automatically calculated by the auxiliary software in the machine was further manually verified with the formula $\triangle P/A \times L/\triangle L$ ($\triangle P$: the compressive force margin of the two points on linear segment of the curve before the first break point; $\triangle L$: the displacement margin of the corresponding two points; A: the area of tested tissue; L: the thickness of tested tissue). As the defects in the control group at 3 months were only filled with small volume of fibrous tissue that further collapsed seriously at 6 months, such biomechanical tests on the regenerated tissue cannot be properly performed as mentioned.

Table 2. Histological Grading Scale for Cartilage Regeneration

Description	*Points*
Cell morphology	
Hyaline cartilage	0
Mostly hyaline cartilage	1
Mostly fibrocartilage	2
Mostly noncartilage	3
Noncartilage only	4
Matrix staining (metachromasia)	
Normal (compared with host adjacent cartilage)	0
Slightly reduced	1
Markedly reduced	2
No metachromatic stain	3
Surface regularity	
Smooth (>3/4)	0
Moderate (>1/2–3/4)	1
Irregular (1/4–1/2)	2
Severely irregular (<1/4)	3
Thickness of cartilage	
>2/3	0
1/3–2/3	1
<1/3	2
Integration of donor with host adjacent cartilage	
Both edges integrated	0
One edge integrated	1
Neither edge integrated	2
Maximum total	14

This table was cited from Wakitani *et al.*'s[20] histological grading scale without modification.

After the biomechanical analysis, GAG contents and COL II determination were performed on the samples collected, as previously reported.[17] First, the samples were rinsed with dd-H_2O, lyophilized for 12 h followed by adding 1 mL cold H_2O and incubated overnight at 4°C in a microcentrifuge tube. After lyses with repeated freeze thawing and sonication cycles, samples were centrifuged at 10,000 rpm for 3 min. The supernatant obtained was subjected to GAG determination, while the precipitates to COL II assay using Native Type II Collagen Detection Kit (Chondrex) according to the manufacturer's instructions.

Since no neo-cartilage was harvested from the control group with scaffold alone, only samples of the experimental group were randomly chosen from five animals for this

analysis at both 3 and 6 months postimplantation. Normal AC in the counterpart from animals at ages equal to those of 3 and 6 months postsurgery (three individuals at each time point), respectively, was employed as a normal control.

Proteome analysis

As previously described,[14,15] the harvested samples for proteome analysis were kept in cold saline for transportation and processed immediately. Both neo-cartilage (sample at 6 months postoperation, $n=5$) and normal cartilage were dissected and extensively washed in cold PBS followed with eventual curettage without any residual blood cells. Tissue samples pulverized were reconstituted in 100 µL digestion buffer (0.1 U chondroitinase ABC [MP Biomedicals], 100 mM Tris acetate, pH 8.0, Mini-protease inhibitor cocktail [Roche Diagnostics]) and incubated for 6 h at 37°C, which was terminated by addition of nine volumes of extraction buffer (4 M guanidine HCl, 50 mM sodium acetate, 65 mM dithiothreitol, 10 mM EDTA, mini-protease inhibitor cocktail). The sample was then sonicated on ice for 10 s 10 times with a 15 s interval in between and centrifuged at 12,000 *g* at 4°C for 1 h to remove proteoglycans and collagens. The supernatant was collected and mixed with three volumes of cold acetone at 20°C overnight to precipitate the proteins. After centrifugation at 12,000 *g* at 4°C for 1 h, the precipitates obtained were thoroughly washed with cold ethanol twice and dissolved in isoelectricfocusing (IEF) rehydration buffer (8 M urea, 2% CHAPS, 18 mM DTT, 0.5% carrier ampholytes, and a trace of bromophenol blue). Protein concentration of each sample was determined by Bradford assay.

For analytic gels, a total of 200ug protein was loaded. The first dimension IEF was run on nonlinear gradient IPG-strips (13 cm, pH 3–10) at 30 V for 12 h, 500 V for 1 h, 1000 V for 1 h, and then 8000 V for 6 h with a limiting current being 50 mA per strip. Strips were sequentially equilibrated in equilibration buffer I (50 mM TriseHCl, pH6.8, 15 mM DTT, 6 M urea, 30% glycerol, 2% sodium dodecyl sulfate [SDS] and a trace of bromophenol blue) and equilibration buffer II (same as buffer I but DTT was replaced by 2.5% iodoacetamide) after IEF completed. Afterward, the second dimension electrophoresis was performed on 12.5% SDS-polyacrylamide gel electrophoresis (PAGE) gels at 30 mA until the bromophenol blue reached the gel bottom. The proteins separated by analytic 2-DE were visualized by silver diamine-staining. While the preparative gels were visualized by a modified coomassie brilliant blue-staining method compatible with MS analysis; data analysis was performed as per protocol. Briefly, the silver-stained 2-DE gels were scanned using a GS710 imaging densitometer (Bio-Rad). Imagemaster software (GE Health Care) was used for spot detection, quantification, and matching.

Statistical analyses

The grading of the macroscopic and histological examination was analyzed using the Mann–Whitney U signed-rank test for Two Independent Samples. GAG content, collagen quantification, and compressive modulus among different groups were analyzed with ANOVA. SPSS 10.0 software was used for statistical analysis and a p-value of <0.05 was considered statistically significant.

Results

Macrographic examination and grading

At 3 months postimplantation, the defects in the experimental group were mostly repaired with engineered cartilage, which exhibited a whitish appearance (Fig. 1A) although the cartilage surface was uneven. While after 6 months, the engineered cartilage became more mature as the joint surface appeared smooth, which bore great similarity in color and texture to the surrounding native cartilage (Fig. 1B). However, a distinguishable border between the

FIG. 1. Gross observation of the articular cartilage repaired postoperation. **(A)** 3 months and **(B)** 6 months of the experimental group, while **(C)** and **(D)** 3 months and 6 months of the control group respectively. Color images available online at www.liebertpub.com/tea

reparative cartilage and surrounding normal tissue still presented even at 6 months postimplantation. In contrast, all defects in the control group were mainly occupied by fibrous tissue with little cartilage-like tissue regenerated at 3 months postimplantation (Fig. 1C). Moreover, the defect became wilder and deeper with the collapse of its adjacent subchondral bone when it reached 6 months postsurgery (Fig. 1D) (For more macroscopic photos, please refer to Supplementary Fig. S1; Supplementary Data are available online at www.liebertpub.com/tea). The corresponding grading of all cases in the experimental and control groups was shown in Table 3. The global macroscopic scores obtained from the experimental group were statistically better than those in the control group.

Histological examination and grading

The histological examination were in consistence with the above observation that the defects of the experimental group at three months postsurgery were repaired by newly generated tissues featured by the formation of lacunas and cell clusters (Fig. 2A), which was characteristic of hyaline cartilage. Besides, the neo-cartilage integrated well with the adjacent cartilage (Fig. 2A and A1) and its underlying subchondral bone (Fig. 2A), although the interface between engineered and normal cartilage can still be identified. However, the cell density remained quite obviously high and cellular arrangement was disordered in the neocartilage (Fig. 2A2). Moreover, the surface was still uneven with penetration of some cartilage-like tissue into the subchondral bone (Fig. 2A).

When it came to 6 months postsurgery, the engineered cartilage become more mature as the neo-tissue was characterized with a cell density and cartilage thickness similar to those of the surrounding native cartilage tissue, including the cartilage surface (Fig. 2B and B1). In addition to those observed in samples at 3 months postoperation, cells in the superficial area of this group exhibited an exclusively single unit and a flat profile parallel to the AC surface (Fig. 2B2). While cells in the deeper zone were observed organized well either in columns or clusters perpendicular to the articular surface (Fig. 2B2). The integration of engineered cartilage with its subchondral bone became more harmonious compared with that of the engineered tissue at 3 months (Fig. 2B vs. Fig. 2A). However, distinct interface was still able to be discriminated (Fig. 2B, 2B1).

On the contrary, the defect in the control group treated with PGA/PLA scaffold alone was only filled with fibrous tissue at 3 months postsurgery (Fig. 2C). Even the surrounding normal cartilage also collapsed to the central regions of the generated fibrous tissue (Fig. 2C1). On the other hand, no residue of the polymeric scaffolding materials in all implanted constructs of the two groups was distinguished as early as 3 months.

According to the histological grading, scores of the experimental group were all significantly better than the corresponding one of the control group as summarized in Table 4. Further comparison of intra-groups shows that the engineered cartilages at 6 months are significantly better than those at 3 months postimplantation (Table 4), indicating that the engineered cartilage underwent a vivid remolding process with postoperation time to gradually enhance its reparative effect.

At the end of 6 months, three of the six samples in the experimental group demonstrated complete regeneration as exhibited in images chosen for figures. In the left three samples, more than 85% of the area was covered with neocartilage. However, only one of six samples in the control group was observed with sparse distribution of fibrocartilage-like tissue regenerated in defects.

Expression of cartilage ECM in engineered cartilage

At 3 months postimplantation, expression of COL II in the engineered cartilage was revealed by IHC staining (Fig. 3A, A1, A2). However, the staining showed uneven distribution of COL II (Fig. 3A2). And there is still distinguishable staining difference between the neighboring normal and engineered cartilage (Fig. 3A1). With the maturation of engineered cartilage, the expression and distribution of COL II was found similar to that of the adjacent native cartilage at 6 months after surgery (Fig. 3B, B1 and B2). However, no expression of COL II was observed in all specimens of the control group in which the defects were occupied by fibrous tissue at either 3 or 6 months (Fig. 3C, D).

Deposition of GAG in the engineered cartilage was confirmed by toluidine blue staining at 3 (Fig. 4A and 4A2) and 6 months (Fig. 4B and 4B2) postsurgery, respectively. The deposition profile of GAG with time is well in consistence with that of COL II. Similarly, little deposition of GAG was detected in the control group after 3 or 6 months (Fig. 4C, D) after implantation.

Biochemical and biomechanical evaluation

The GAG deposition and COL II expression of engineered cartilage was further quantified by biochemical analysis and

Table 3. Results of Grading Scale for Gross Appearance

	3 Months (n = 6)		*6 Months* (n = 6)	
Grading	*Exp*	*Cont*	*Exp*	*Cont*
Intraarticular adhesions	1.3 (1–2)	0.43 (0–1)	1.3 (1–2)	0.14 (0–1)
Restoration of articular surface	1.5 (1–2)	0.57 (0–1)	1.5 (1–2)	0.42 (0–1)
Erosion of cartilage	1.3 (1–2)	0.57 (0–1)	1.5 (1–2)	0.42 (0–1)
Appearance of cartilage	1.0 (0–2)	0.28 (0–1)	1.5 (1–2)	0.14 (0–1)
Total	5.2 (3–6)[a]	1.86 (1–3)	5.8 (5–8)[a,b]	1.14 (1–2)

Each data represent mean and range (parentheses) of the scales.
[a] $p < 0.01$, versus the control group.
[b] $p < 0.05$, versus the experimental group of 3M.
Exp, experimental group; Cont, control group.

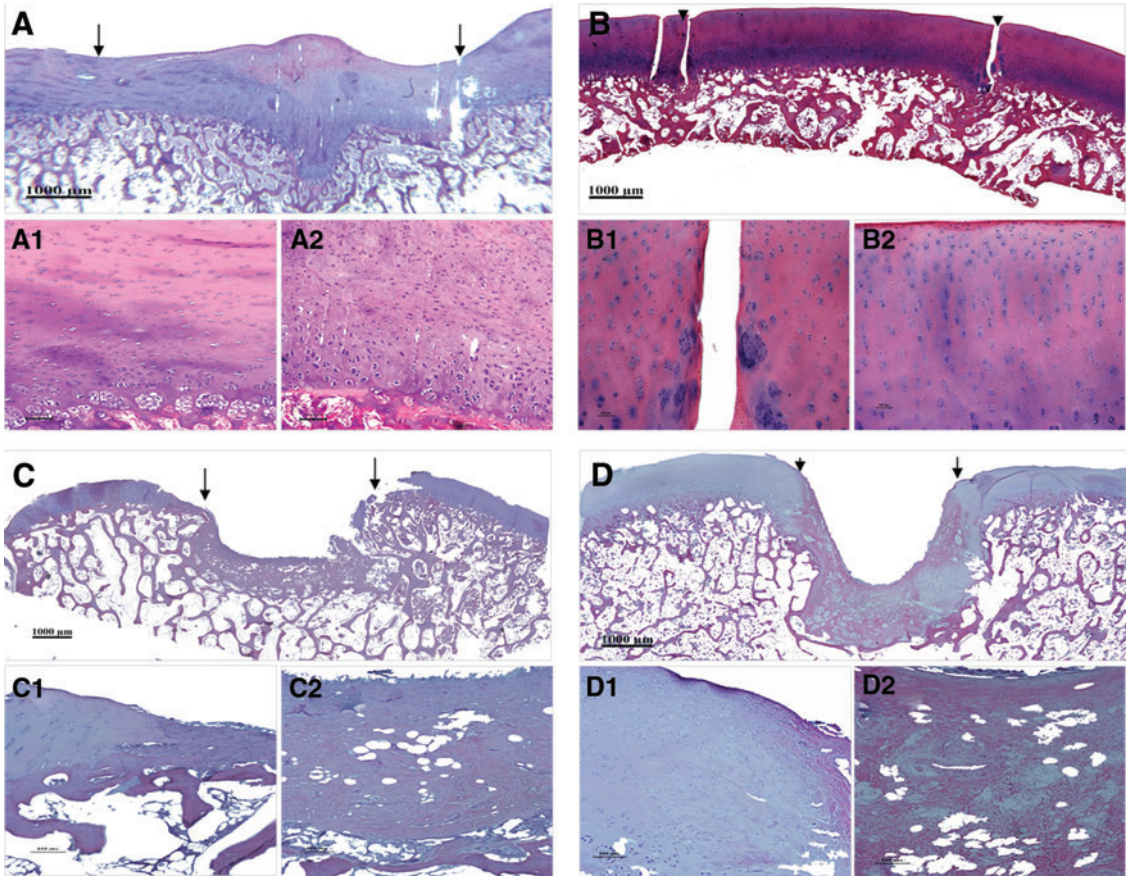

FIG. 2. Hematoxylin and eosin staining of the regenerated tissue at 3 and 6 months postimplantation. **(A)** Regeneration of neo-cartilage at 3 months postsurgery. **(B)** At 6 months after repairing, defect in the experimental group was repaired with hyaline cartilage. **(C)** Defect in the control group (PGA/PLA scaffold alone) was filled with little fibrous tissue and the adjacent normal cartilage collapsed at 3 months postimplantation. **(D)** Collapse of subchondral bone occurred in the control group after 6 months of repairing. The reparative area was indicated by arrowheads or arrows. **(A1)**, **(B1)**, **(C1)**, and **(D1)** are high-magnification images of the interface between the repaired tissue and adjacent normal cartilage while **(A2)**, **(B2)**, **(C2)**, and **(D2)** are central area of reparative tissue in full thickness from superficial cartilage to subchondral bone. (Bar scales: 1000 μm for **A, B, C,** and **D**; 100 μm for others.) Color images available online at www.liebertpub.com/tea

also compared with that of the normal one. As is shown (Fig. 5A, B), the amount of GAG in the engineered cartilage at 3 months reached nearly 80% ($p<0.05$) of that in the corresponding normal cartilage, while collagen type II rearched 70% ($p<0.05$). However, with the maturation of engineered cartilage till 6 months, GAG content in the regenerated cartilage was increased reaching 90% of that in corresponding native cartilage ($p<0.05$) (Fig. 5A), while collagen type II almost same as native cartilage ($p<0.05$) (Fig. 5B).

The biomechanical property of the engineered cartilage was estimated by measuring its compressive modulus, which was also compared with that of the normal one at the

Table 4. Results of Histological Grading for Cartilage Regeneration

	3 Months (n=6)		*6 Months (n=6)*	
Grading	*Exp*	*Cont*	*Exp*	*Cont*
Cell morphology	0.8 (1–3)	2.29 (2–3)	0.7 (0–2)	3.43 (2–4)
Matrix staining	0.8 (0–2)	1.43 (1–2)	0.7 (0–2)	2.57 (2–3)
Surface regularity	1.3 (0–2)	2.43 (2–3)	0.5 (0–1)	2.57 (2–3)
Thickness of cartilage	0.8 (0–1)	1.43 (1–2)	0.3 (0–1)	1.71 (1–2)
Integration with host cartilage	1.3 (0–1)	1.14 (0–2)	0.3 (0–1)	1.71 (1–2)
Total	5.0 (4–8)[a]	8.71 (7–11)	2.5 (2–5)[a,b]	12.00 (8–14)

Each data represent mean and range (parentheses) of the scales.
[a]$p<0.01$, versus the control group.
[b]$p<0.05$, versus the experimental group of 3M.

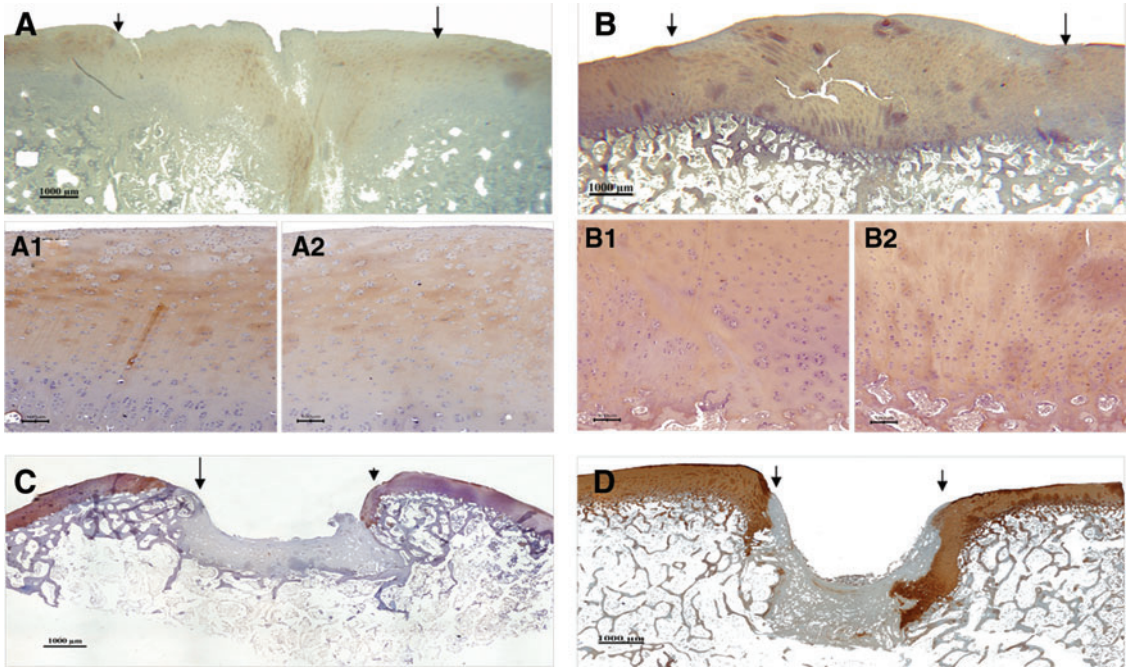

FIG. 3. Immunohistochemical staining for collagen type II in reparative tissue at 3 and 6 months postimplantation respectively. The arrows or arrowheads indicate the interface between the reparative tissue and adjacent host cartilage. **(A)** 3 months and **(B)** 6 months after surgery in experimental group. **(A1)** and **(B1)** are high-magnification of interface between neocartilage and the native one while **(A2)** and **(B2)** are that from central area of reparative tissue in full thickness from superficial cartilage to subchondral bone. **(C)** 3 months and **(D)** 6 months after surgery in the control group. (Bar scales: 1000 μm for **A, B, C, and D**; 100 μm for **A1, A2, B1,** and **B2.**). Color images available online at www.liebertpub.com/tea

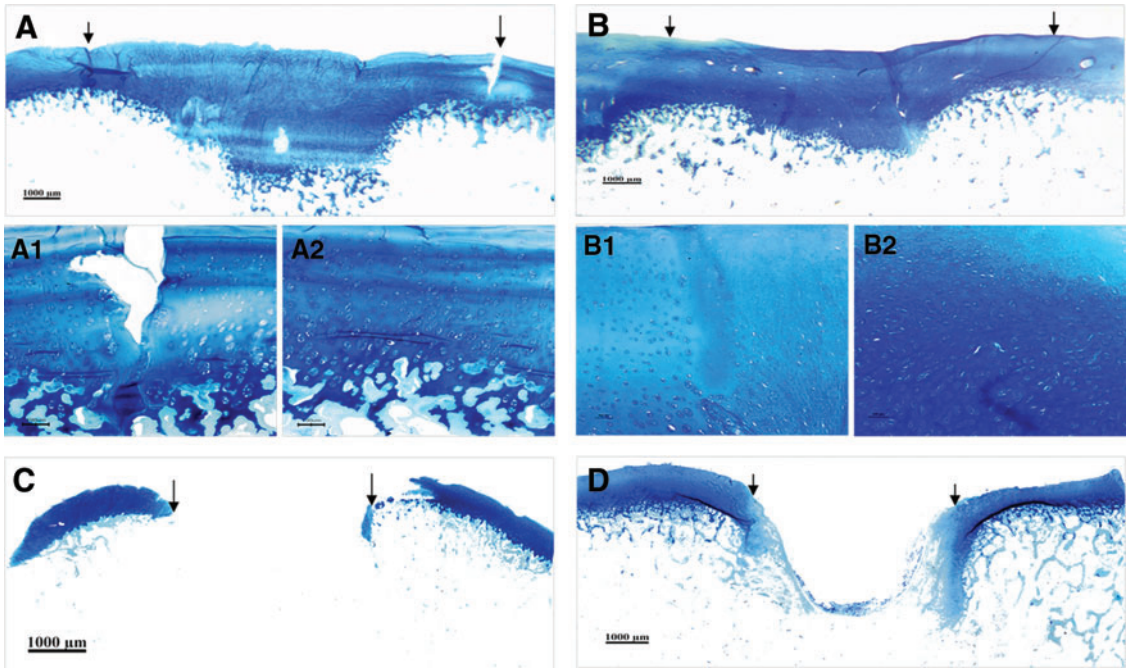

FIG. 4. Toluidine blue staining of repaired tissue. **(A)** At 3 months postsurgery, repaired tissue showed deposition of glycosaminoglycans (GAG) in experimental group. **(B)** At 6 months after surgery, distribution of GAG in repaired cartilage exhibited in a similar way as that in native ones in experimental group. **(A1 and B1)** are high magnification of the interface while **(A2 and B2)** are high-magnification views of central area of reparative tissue in **(A)** and **(B)**. Little deposition of GAG could be detected in the defect area of the control group at 3 **(C)** and 6 months **(D)** postsurgery (Bar scales: 1000 μm for **A, B, C, and D**; 100 μm for **A1, A2, B1, and B2**). The arrows or arrowheads indicate the interface between the reparative tissue and adjacent host cartilage. Color images available online at www.liebertpub.com/tea

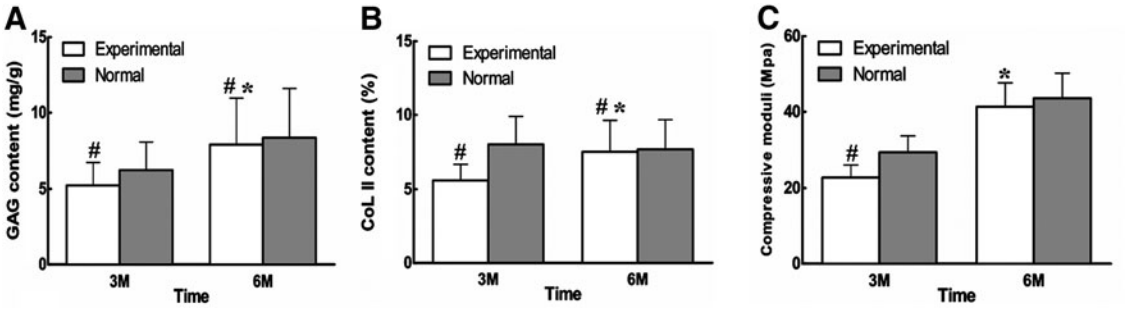

FIG. 5. Biochemical and biomechanical analysis of the engineered cartilage **(A)** The GAG content of the reparative cartilage. The amount of GAG in the engineered cartilage at 3 months reached nearly 80% ($p < 0.05$) of that in the corresponding normal cartilage, while that of 6 months increased to almost 90% of the native cartilage ($p < 0.05$). **(B)** The collagen type II deposition of the reparative cartilage. Collagen type II reached 70% ($p < 0.05$) of the native cartilage at 3 months while almost same as native cartilage 6 months postoperation ($p < 0.05$). **(C)** The biomechanical property of the reparative cartilage. The compressive modulus of the neo-cartilage at 3 months postimplantation reached 70% of that of the normal cartilage ($p < 0.05$) while that at 6 months to 90%, but without statistical significance ($p > 0.05$). A significant increase in GAG content, collagen content, and compressive moduli of engineered cartilage at 6 months postrepair was observed compared with those of 3 months ($p < 0.05$) (*means significantly different compared with engineered cartilage at 3 months; #, means significantly different compared with the corresponding normal cartilage).

similar age. At 3 months postoperation, the compressive modulus of engineered cartilage reached more than 70% of that of the normal cartilage ($p < 0.05$), while at 6 months postoperatively, it increased to reach nearly 90% albeit without significant difference between the values of the engineered and normal cartilage ($p > 0.05$) (Fig. 5C). These results suggested that remodeling in both histology and biochemistry constantly occurred with repairing time increase, which is usually required for the recovery of AC not only structurally but also functionally.

Proteome analysis

Proteins extracted from engineered and normal AC were separated respectively via IEF as the first dimension and SDS-PAGE as the second dimension electrophoresis prior to silver diamine-staining. Scanned gels were analyzed using ImageMaster 2D Platinum5.0 software. The experiments were carried out in triplicate to ensure reproducibility of samples in 2-D gels. Analysis of protein profiles from two different samples by 2D gels (pH 3–10) was performed (Fig. 6). Totally 20 protein spots were selected to be detected in gels from normal and engineered cartilage samples, respectively. These differentially expressed proteins were considered for protein identification by peptide mass fingerprinting. Proteins were considered definitely present if the searched results showed at least two matched peptides per protein. Of these analyzed spots, 43 proteins were identified between groups, of which 16 proteins were found to be differentially expressed in engineered cartilage in comparison to normal one by MS analysis and database searching. Protein expression patterns are shown in Table 5, in which

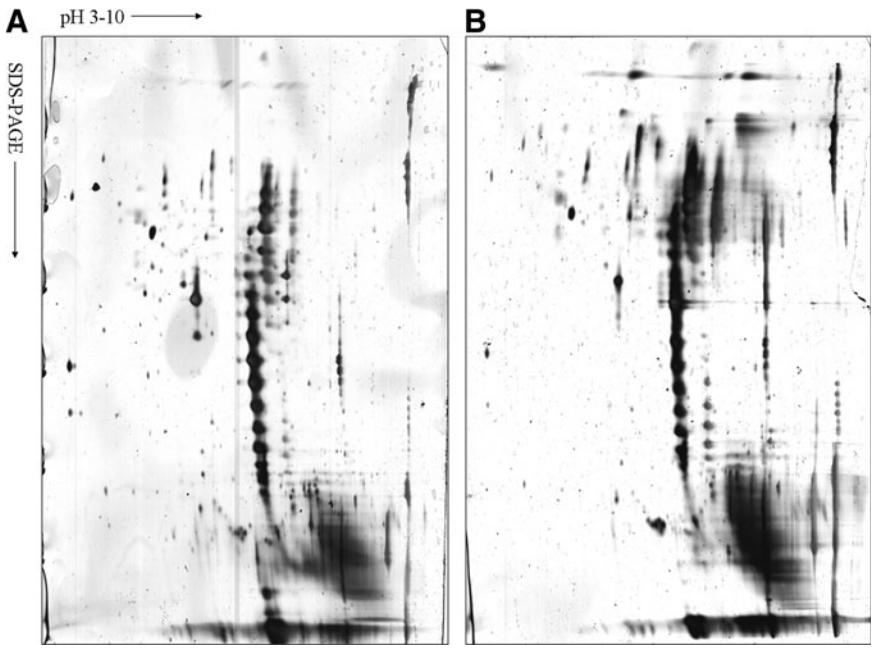

FIG. 6. Typical protein profiles of 2D PAGE for tissue-engineered cartilage constructed by ASCs and normal porcine cartilage. Three 2-D electrophoresis gels after silver staining are shown here as representatives. **(A)** Tissue-engineered cartilage of 6 months; **(B)** normal cartilage served as positive control. Identified proteins are listed in Table 5. Horizontal axes designate the pH value, and vertical axes designate molecular mass.

Table 5. Differential Expression of Proteins Identified from Normal and Engineered Cartilage

Dot no.	Distinct peptides	Distinct summed MS/MS search score	AA% coverage	UniProt	Protein name	Functional classification
2	2	29.24	6	O11780	Transforming growth factor-beta-induced protein ig-h3 precursor	Collagen assembly protien/cell adhesion
4	9	141.89	17	P09571	Serotransferrin	Metal binding
5	2	29.09	4	P09571	Serotransferrin	Metal binding
6	2	32.6	8	Q5S1S4	Carbonic anhydrase 3	Metal binding
7	4	60.87	22	Q5S1S4	Carbonic anhydrase 3	Metal binding
9	3	44.46	21	P00761	Trypsin precursor	Enzyme
11	2	36.07	14	Q8MK67	Phosphatidylethanolamine-binding protein 1	Binding protein/ATP binding
15	2	29.8	1	P28481	Collagen alpha-1(II) chain precursor	Structural constituent
17	3	50.06	19	P51779	Complement factor D precursor	Enzyme/immunity
18	2	41.26	7	Q1KYT0	Beta-enolase	Glycolysis
	4	76.87	16	Q9XSJ4	Alpha-enolase	Glycolysis
	2	40.29	9	P42897	Enolase	Glycolysis
20	6	104.71	14	P19120	Heat shock cognate 71 kDa protein	Transcription/ATP binding
	2	36.64	4	Q6BZH1	78 kDa glucose-regulated protein homolog precursor	Protein assembly/ATP binding
	2	33.46	4	P08108	Heat shock cognate 70 kDa protein	Protein assembly/ATP binding
	2	32.89	3	P08418	Heat shock 70 kDa protein homolog	Protein assembly/ATP binding
	2	31.99	3	P29843	Heat shock 70 kDa protein cognate 1	Microtubule assembly
	2	34.06	12	P00761	Trypsin precursor	Enzyme
21	2	31.19	7	Q1KYT0	Beta-enolase	Glycolysis
	4	66.94	14	Q9XSJ4	Alpha-enolase	Glycolysis
	3	52.57	11	P42897	Enolase	Glycolysis
	3	46.55	9	Q9W7L1	Alpha-enolase	glycolysis
	2	32.18	6	O57391	Gamma-enolase	Glycolysis
22	8	136.92	24	P79385	Lactadherin	Cell adhesion/angiogenesis
	3	54.87	11	P19140	Alpha-enolase	Glycolysis
	2	39.83	9	P42897	Enolase	Glycolysis
	2	33.93	6	Q05524	Alpha-enolase, lung specific	Glycolysis
23	3	52.25	13	P19620	Annexin A2	Metal binding
	2	31.67	10	O62823	Alpha-S1-casein precursor	Antioxidant
24	2	25.32	8	P20112	SPARC precursor	Angiogenesis/sinal transduction
25	2	27.35	5	P20305	Gelsolin precursor	Actin binding protein/apoptosis
27	5	80.14	19	O15335	Chondroadherin precursor	Collagen assembly protien
31	3	56.56	26	P80031	Glutathione S-transferase P	Metabolism
32	2	30.37	1	P20908	Collagen alpha-1(V) chain precursor	Structural constituent
33	2	31.47	12	Q9GKQ6	Biglycan precursor	Collagen fiber assembly
	2	41.81	1	P05539	Collagen alpha-1(II) chain precursor	Structural constituent
35	3	57.51	16	Q29371	Triosephosphate isomerase	Glycolysis
36	2	33.89	3	P08835	Serum albumin precursor	Metal binding/apoptosis
38	3	50.62	12	P79385	Lactadherin	Cell adhesion/angiogenesis
39	4	54.87	8	P30101	Protein disulfide-isomerase A3 precursor	Antioxidant/metabolism/apoptosis
	2	23.89	20	P81605	Dermcidin precursor	Antimicrobial activity
40	7	120.33	33	P08758	Annexin A5	Ca2 mediator/anti-apoptosis
	2	32.13	7	O15335	Chondroadherin precursor	Collagen assembly protien

serial identified proteins with their respective spot ID, protein name, number of matched peptides, percentage of sequence coverage, MS/MS search score, and functional classification are included.

Proteins differentially identified in Table 5 are grouped according to their biological function or their cellular role on the basis of annotations from the UniProt Knowledgebase (www.ebi.uniprot.org/index.shtml). A graphical representation of the identified proteins categorized by function is shown in Figure 7, among which the largest group comprised of 15 proteins functions as cellular organization relative protein, chiefly for cytoskeleton relative and ECM assembly. The former group includes HSP, gelsolin, and annexin while the latter one comprises TGF-β ip ig-h3, collagen type II/V, protein disulfide isomerase A3, biglycan, and chondroadherin. It is also revealed that enolase family members such as alpha-enolase, beta-enolase, and gamma-enolase are differentially identified, whose role is to take part in glucose metabolism for energy supply. Besides, differential analysis also discloses proteins involving in signal

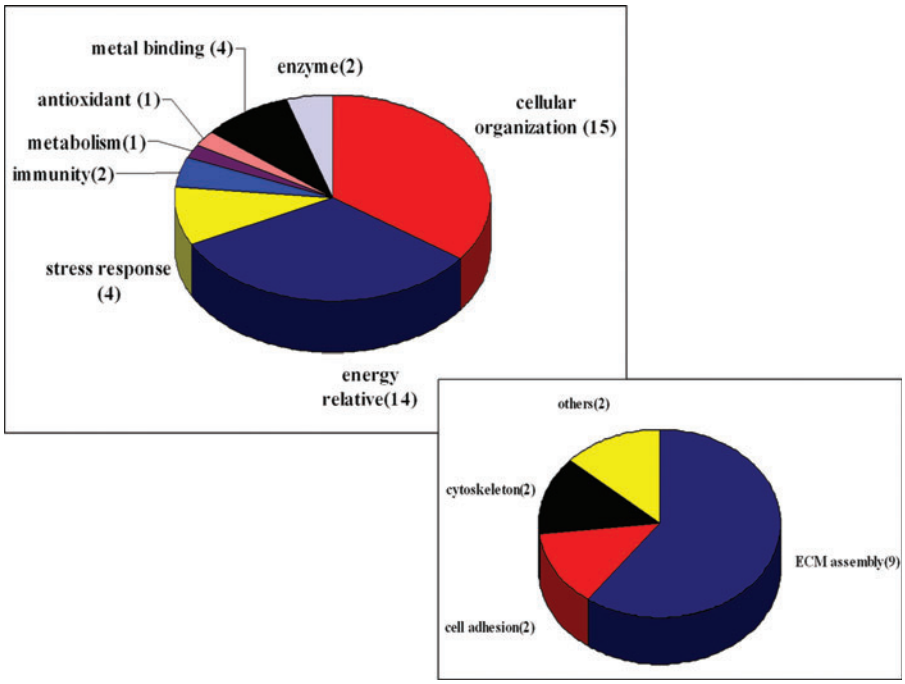

FIG. 7. Distribution and functional classification of proteins identified by 2-DE and MS from engineered and native cartilage. Distribution of all identified proteins is categorized according to their annotation in the UniProt Knowledgebase while the smaller frame shows subclasses of cellular organization. Color images available online at www.liebertpub.com/tea

transduction as HSP71 and SPARC, and proteins as triosephosphate isomerase and glutathione S-transferase P dedicated to metabolism, while other proteins belong to metabolism, signal transduction, antioxidant, antimicrobials, and enzyme activity, respectively.

In addition, proteins with unknown functions in cartilage such as alpha-S1-casein precursor, protein disulfide-isomerase A3 precursor, dermcidin precursor, and complementary system member such as complement factor D precursor are also differentially identified in this study.

Discussion

In our previous study, utilizing chondrogenesis-induced ASCs and PGA fibers as scaffold, we have successfully repaired defects created in nonweight-bearing area of AC in a porcine model. However, compared to cartilage from nonweight-bearing area, cartilage regeneration at weight-bearing area has higher requirement. First, for the weight-bearing area is tightly connected to the other structures in the knee joint (such as meniscus), a sufficient exposure of this area in operation is critical for implantation and fixation of cell scaffold. On the other hand, more exposure would lead to more impairment to the integrity of the joint. Thus, we exposed the weight-bearing area with subluxation of joint to reduce the damage to the joint integrity. Second, secure fixation of cell-scaffold construct is critical for generation of engineered cartilage. According to Knecht *et al.*,[18] we stabilized the engineered cartilage by two crossed transosseous fixation using biodegradable sutures and no dislocation of the complex was observed in the following study.

Besides, compared with nonweight-bearing area, restoration of defects within weight-bearing area is more important for clinical practice.[21–23] Functionally, weight-bearing area cartilage is the major structure in knee joint that is responsible for compression transmission and absorption.[24] It has been demonstrated that more than 80% of patients suffering full thickness defects within weight-bearing areas may progress into osteoarthritis within 5–10 years.[25] However, up to now, most of data regarding *in vivo* regeneration of AC comes from results in small animal model including rodent and rabbits. Thus, the question remained to be answered whether ASCs would heal weight-bearing cartilage defects in an animal model, which is comparable in body weight, size of knee joint, and AC structure to that in human beings. As reported by Shepherd *et al.*, the average thickness of weight-bearing cartilage in human knee ranges from 1.65 to 2.65 mm,[26] similar to the 1.5 cm thickness in porcine model used in this study. Thus, a full-thickness AC defect was created in weight-bearing area in porcine model to investigate whether regenerated cartilage from ASCs share structure and molecular characteristics similar to that of normal cartilage. Therefore, it is of great importance to perform the present study on full-thickness defects repair in weight-bearing area considering its role in the joint.

In the present study, full-thickness defects in weight-bearing area were repaired with chondrogenic differentiated ASCs loaded on PGA/PLA scaffold with a follow-up of 3 months and 6 months. Histologically, the neo-generated tissue exhibited high cell density, and disordered orientation at 3 months. While after 6 months, density and organization of cells within the engineered cartilage remodeled into a similar pattern as that in surrounding normal tissue. Meanwhile, from 3 to 6 months after transplantation, content of GAG increased from 80% to 90%, while COL II from 70% to almost the same as that of the native cartilage, respectively. Additionally, compress modulus of regenerated cartilage improved from 70% to 90% of that of normal ones, indicating a structural remodeling process occurred with function improvement. As to biomechanics, this actually was functional reflection of its structure. However, all these accumulating data suggest that differences are still present between the engineered and native cartilage. In the present study totally 43 differential proteins were identified between the

regenerated and native cartilage utilizing proteome and mass spectrometry (Fig. 7 and Table 5) analysis. To our knowledge, no such study has been found about proteomic profile of tissue-engineered cartilage generated in weight-bearing areas in a large animal model.

Cartilage is well organized tissue with chondrocytes sparsely distributed in extreme abundant self-secreted ECM, chiefly comprising collagenous and noncollagenous matrix such as proteoglycans. According to the histological examination (Fig. 2B), regenerated cartilage was recognized by formation of lacuna and cell cluster in structure, and expression of GAG and COL II in component (Fig. 3B, 4B), indicating that defects in weight-bearing area of AC has been repaired with hyaline-like cartilage. However, in most of the reports including ours, which attempted to heal cartilage defect using MSCs, the engineered cartilage was frequently inferior to the native ones in tissue structure, ECM component, and biomechanical properties. As a major component in cartilage, COL II has been proved to be the most important element in maintaining structure integrity and tensile strength of cartilaginous matrix. After 6 months, we found that COL II deposition in engineered cartilage reached 97% of that in native ones. Such a little difference with no statistical significance cannot account for the inferiority of restored cartilage in tissue structure and tensile strength. Moreover, fibrillogenesis of collagen is to a great extent determined by other macromolecules alloyed into D-periodically banded fibrils. Biglycan and chondroadherin are such leucine-rich small proteoglycans involved in collagen synthesis. Belonging to one subfamily, biglycan was found ubiquitously with decorin in a variety of tissue including cartilage, which was documented to participate in ECM assembly[27] and tissue organization in response to growth factors and cytokines.[27,28] Chondroadherin was found involved in isolated chondrocytes adhesion and chondrocyte growth and proliferation via integrins $\alpha 2\beta 1$.[29,30] Thus, their contribution to ECM is not only indirectly restricted to collagen assembly, but also direct participation included. Especially those like chondroadherin, they act as a bridge via integrins between cytoskeleton and ECM to make cartilage function as a whole in multiple cellular events.[31–34] TGF-β ip ig-h3 has been demonstrated by Tran T to be implicated in mediating cell adhesion and migration[35] via binding to collagen type I, II, and IV, which is increased response to TGF-β treatment,[36] the media utilized in our chondrogenic system. In addition to ECM synthesis relative proteins, protein disulfide isomerase A3 involved in cartilage oligomeric matrix protein (COMP) metabolism was also identified with lower expression in engineered cartilage. As is known, COMP is a type of a large pentameric glycoprotein and member of the thrombospondin (TSP) group located in the territorial matrix of chondrocytes, whose abnormal expression has been demonstrated closely related to skeletal dysplasia.[37,38] The identification of protein disulfide isomerase A3, one multifunctional protein resident in the lumen of the endoplasmic reticulum, may remind us of abnormality in COMP metabolism in our engineered cartilage.

As differentiation of ASCs toward chondrocytes is the premise to the regeneration of hyaline cartilage, whether grafted ASCs could maintain their committed chondrogenic phenotype is of first consideration. Correspondingly, proteins mediating chondrocytes differentiation such as cartilage-specific ECM proteins, SPARC, and annexin V were differentially identified in proteomic analysis. In addition to their role in maintaining structure of cartilage, newly deposited ECM has been reported to participate in the regulation of chondrogenic phenotype through cell shape control. As reported by Lu *et al.*,[39] COL II provides the inductive signaling for chondrogenic differentiation in ASCs by evoking a round cell shape through integrin β1-mediated Rho A/Rock signaling pathway. Known initially as bone protein, SPARC (osteonectin), which secreted acidic protein rich in cysteine, has been mainly identified in chondrocyte of both developing cartilage and adult bone. Whereas SPARC mRNA was abundant in chondrocytes of the upper hypertrophic and proliferative zones, SPARC protein was detected extracellularly only in the zone of mineralized cartilage. On the other hand, SPARC has been recognized in contribution to the organization of matrix by binding to a number of different ECM components including fibrillar collagens (types I, II, III, and V) and collagen type IV. And also, SPARC has been appreciated as a cell shape modifier that modulates cellular proliferation, migration, and differentiation.[40] Its role in trafficking of cartilage ECM has been indicated by the observation that retention of SPARC in the endoplasmic reticulum coincided with COMP.[41] As to annexin V, it has been documented that annexin-mediated Ca21 influx into chondrocytes of growth plate was a positive regulator of terminal differentiation.[34,42–44] In summary, the presence of these proteins implicated in chondrocyte differentiation further indicates the success of our engineering. On the contrary, the reason why there is gap between the neocartilage we engineered and the native one possibly lies in the differentiation of ASCs toward chondrocytes *per se*. Therefore, these mentioned factors influencing chondorgenic differentiation are to provide facilitation for our engineering.

Normally, chondrocytes resided in AC survived and maintained tissue integrity in an avascular, hypoxic environment. Oxygen tension gradient exposed to AC was reported to be 7% in the articular surface while 1% in the deeper layer.[45] Thus, with the absence of sufficient oxygen supply, chondrocytes have to resort to glycolysis[46–48] rather than oxidative phosphorylation for ATP production, accounting for approximately 95% of their energy consumption. As a key player in glycolysis, enolase family including $\alpha/\beta/\gamma$ subunits is responsible for the reversible conversion of the D-2-phosphoglycerate (2PGA) and phosphoenolpyruvate (PEP) in glycolysis and gluconeogenesis, two metabolic pathways that are often vital for cellular function. Physiologic generation of ATP by chondrocytes supports and chondrocyte viability and collagen synthesis, and the formation of phosphoadenosine sulfate, which is involved as a sulfate donor in the synthesis of sulfated proteoglycans (PGs). In the present study, 11 of 43 proteins referred to enolase family, which are differentially expressed in engineered cartilage compared with that in normal ones. Thus, lower expression of enolase family may heavily influence energy stores of implanted ASCs and further undermine repair activities of engineered cartilage even after 6 months. In line with this result, proteins related to glycolysis were found to be the largest group differentially identified in OA cartilage,[49] which is characterized by decreased synthesis of cartilage ECM. In addition to its role in biosynthesis of

chondrocytes, glycolysis has been reported to take part in chondrogenic differentiation of MSCs. MSCs cultured under low oxygen tension have been found to increase the cartilage-specific ECM synthesis including GAGs and COL II,[50] although controversies still exist.[51] Further study revealed that MSCs differentiated toward the chondrogenic lineage had significantly reduced oxygen consumption, indicating a shift toward a predominantly glycolytic metabolism. Therefore, differentially decreased expression of enolase family in engineered cartilage indicated a reduced glycolytic pathway in implanted ASCs, which would further interfere with its chondrogenic differentiation *in vivo*. Taken together, this result could partially explain why engineered cartilage always showed fundamental distinctions with native ones in structure, composition, and mechanical strength.

Conclusion

In summary, the present study demonstrated the possibility of AC repair in weight-bearing area with chondrogenic differentiated autologous ASCs seeded on PGA/PLA scaffold in porcine model. Although the cartilage repair in the porcine model was confirmed by the ECM accumulation including GAG and COL II and biomechanical modulus, difference between the engineered and native cartilage was further disclosed by proteome profile analysis, by which 43 differentially identified proteins could be categorized into four functional groups: glycolysis, cellular organization, signaling pathway, and others. These results are to either provide a better understanding of the profiles of protein responsible for the formation of engineered cartilage or be helpful for further exploring mechanical clues why engineered cartilage are always similar but not the same as native ones.

Acknowledgment

This study is financially supported by the Natural Science Foundation of China (Grant no: 30970743, Grant no: 81201204, and Grant no: 81271724).

Disclosure Statement

No competing financial interests exist.

References

1. Alford, J.W., and Cole, B.J. Cartilage restoration, part 1. Basic science, historical perspective, patient evaluation and treatment options. Am J Sports Med **33,** 295, 2005.
2. Serra, C.I., Soler, C., Carillo, J.M., Sopena, J.J., Redondo, J.I., and Cugat, R. Effect of autologous platelet-rich plasma on the repair of full-thickness articular defects in rabbits. Knee Surg Sports Traumatol Arthrosc **21,** 1730, 2013.
3. Evans, C.H., Ghivizzani, S.C., and Robbins, P.D. Orthopedic gene therapy in 2008. Orthopedic gene therapy in 2008. Mol Ther **17,** 231, 2009.
4. Zuk, P.A., Zhu, M., Mizuno, H., Huang, J., Futrell, J.W., Katz, A.J., Benhaim, P., Lorenz, H.P., and Hedrick, M.H. Multilineage cells from human adipose tissue: implications for cell based therapies. Tissue Eng **7,** 211, 2001.
5. Zuk, P.A., Zhu, M., Ashjian, P., De Ugarte, D.A., Huang, J.I., Mizuno, H., Alfonso, Z.C., Fraser, J.K., Benhaim, P., and Hedrick, M.H. Human adipose tissue is a source of multipotent stem cells. Mol Bio Cell **13,** 4279, 2002.
6. De Ugarte, D.A., Morizono, K., Elbarbary, A., Alfonso, Z., Zuk, P.A., Zhu, M., Dragoo, J.L., Ashjian, P., Thomas, B., Benhaim, P., Chen, I., Fraser, J., and Hedrick, M.H. Comparison of multi-lineage cells from human adipose tissue and bone marrow. Cells Tissues Organs **174,** 101, 2003.
7. Zheng, B., Cao, B., Li, G., and Huard, J. Mouse adipose-derived stem cells undergo multilineage differentiation *in vitro* but primarily osteogenic and chondrogenic differentiation *in vivo*. Tissue Eng **12,** 1891, 2006.
8. Dragoo, J.L., Lieberman, J.R., Lee, R.S., Deugarte, D.A., Lee, Y., Zuk, P.A., Hedrick, M.H., and Benhaim, P. Tissue engineered bone from BMP-2-transduced stem cells derived from human fat. Plast Reconstr Surg **115,** 1665, 2005.
9. Kim, J., Kim, S.H., Lee, S.U., Ha, G.H., Kang, D.G., Ha, N.Y., Ahn, J.S., Cho, H.Y., Kang, S.J., Lee, Y.J., Hong, S.C., Ha, W.S., Bae, J.M., Lee, C.W., and Kim, J.W. Proteome analysis of human liver tumor tissue by two-dimensional gel electrophoresis and matrix assisted laser desorption/ionization-mass spectrometry for identification of disease-related proteins. Electrophoresis **23,** 4142, 2002.
10. Chen, J., Kahne, T., Rocken, C., Gotze, T., Yu, J., Sung, J.J., Chen, M., Hu, P., Malfertheiner, P., and Ebert, M.P. Proteome analysis of gastric cancer metastasis by two-dimensional gel electrophoresis and matrix assisted laser desorption/ionization-mass spectrometry for identification of metastasis-related proteins. J Proteome Res **3,** 1009, 2004.
11. Lee, I.N., Chen, C.H., Sheu, J.C., Lee, H.S., Huang, G.T., Yu, C.Y., Lu, F.J., and Chow, L.P. Identification of human hepatocellular carcinoma-related biomarkers by two-dimensional difference gel electrophoresis and mass spectrometry. J Proteome Res **4,** 2062, 2005.
12. Domon, B., and Aebersold, R. Mass spectrometry and protein analysis. Science **312,** 212, 2006.
13. Aebersold, R. A mass spectrometric journey into protein and proteome research. J Am Soc Mass Spectrom **14,** 685, 2003.
14. Ruiz-Romero, C., López-Armada, M.J., and Blanco, F.J. Proteomic characterization of human normal articular chondrocytes: a novel tool for the study of osteoarthritis and other rheumatic diseases. Proteomics **5,** 3048, 2005.
15. Vincourt, J.B., Lionneton, F., Kratassiouk, G., Guillemin, F., Netter, P., Mainard, D., and Magdalou J. Establishment of a reliable method for direct proteome characterization of human articular cartilage. Mol Cell Proteomics **5,** 1984, 2006.
16. Valina, C., Pinkernell, K., Song, Y.H., Bai, X., Sadat, S., Campeau, R.J., Le Jemtel, T.H., and Alt, E. Intracoronary administration of autologous adipose tissue-derived stem cells improves left ventricular function, perfusion, and remodelling after acute myocardial infarction. Eur Heart J **28,** 2667, 2007.
17. Cui, L., Wu, Y., Cen, L., Zhou, H., Yin, S., Liu, G., Liu, W., and Cao, Y. Repair of articular cartilage defect in non-weight bearing areas using adipose derived stem cells loaded polyglycolic acid mesh. Biomaterials **30,** 2683, 2009.
18. Knecht, S., Erggelet, C., Endres, M., Sittinger, M., Kaps, C., and Stüssi, E. Mechanical testing of fixation techniques for scaffold-based tissue-engineered grafts. J Biomed Mater Res B Appl Biomater **83,** 50, 2007.
19. Cook, S.D., Patron, L.P., Salkeld, S.L., and Rueger, D.C. Repair of articular cartilage defects with osteogenic protein-1 (BMP-7) in dogs. J Bone Joint Surg Am **85-A (Suppl. 3),** 116, 2003.

20. Wakitani, S., Goto, T., Pineda, S.J., Young, R.G., Mansour, J.M., Caplan, A.I., and Goldberg, V.M. Mesenchymal cell-based repair of large, full-thickness defects of articular cartilage. J Bone Joint Surg Am **76,** 579, 1994.
21. Dragoo, J.L., Carlson, G., McCormick, F., Khan-Farooqi, H., Zhu, M., Zuk, P.A., and Benhaim, P. Healing full-thickness cartilage defects using adipose-derived stem cells. Tissue Eng **13,** 1615, 2007.
22. Liu, Y., Chen, F., Liu, W., Cui, L., Shang, Q., Xia, W., Wang J, Cui Y, Yang G, Liu, D., Wu, J., Xu, R., Buonocore, S.D., and Cao, Y. Repairing large porcine full-thickness defects of articular cartilage using autologous chondrocyte-engineered cartilage. Tissue Eng **8,** 709, 2002.
23. Nehrer, S., and Minas, T. Treatment of articular cartilage defects. Invest Radiol **35,** 639, 2000.
24. Maquet, P.G., Van de Berg, A.J., and Simonet, J.C. Femorotibial weightbearing areas. Experimental determination. J Bone Joint Surg Am **57,** 766, 1975.
25. Hangody, L., and Módis, L. Surgical treatment options for weight bearing articular surface defect. Orv Hetil **147,** 2203, 2006.
26. Shepherd, D.E., and Seedhom, B.B. Thickness of human articular cartilage in joints of the lower limb. Ann Rheum Dis **58,** 27, 1999.
27. Svensson, L., Oldberg, A., and Heinegård, D. Collagen binding proteins. Osteoarthritis Cartilage **S23,** 9 Suppl A, 2001.
28. Iozzo, R.V. The biology of the small leucine-rich proteoglycans. Functional network of interactive proteins. J Biol Chem **274,** 18843, 1999.
29. Camper, L., Heinegârd, D., and Lundgren-Akerlund, E. Integrin alpha2beta1 is a receptor for the cartilage matrix protein chondroadherin. J Cell Biol **138,** 1159, 1997.
30. Shen, Z., Gantcheva, S., Månsson, B., Heinegârd, D., and Sommarin, Y. Chondroadherin expression changes in skeletal development. Biochem J **330 (Pt 1),** 549, 1998.
31. Schwartz, M.A., Schaller, M.D., and Ginsberg, M.H. Integrins: emerging paradigms of signal transduction. Annu Rev Cell Dev Biol **11,** 549, 1995.
32. Clancy, R.M., Rediske, J., Tang, X., Nijher, N., Frenkel, S., Philips, M., and Abramson, S.B. Outside-in signaling in the chondrocyte. Nitric oxide disrupts fibronectin-induced assembly of asubplasmalemmal actin/rho A/focal adhesion kinase signaling complex. J Clin Invest **100,** 1789, 1997.
33. Wang, W., and Kirsch, T. Annexin V/beta5 integrin interactions regulate apoptosis of growth plate chondrocytes. J Biol Chem **281,** 30848, 2006.
34. Hirsch, M.S., Lunsford, L.E., Trinkaus-Randall, V., and Svoboda, K.K. Chondrocyte survival and differentiation *in situ* are integrin mediated. Dev Dyn **210,** 249, 1997.
35. Tran, T., Gosens, R., and Halayko, A.J. Effects of extracellular matrix and integrin interactions on airway smooth muscle phenotype and function: it takes two to tango! Curr Respir Med Rev **3,** 193, 2007.
36. Hashimoto, K., Noshiro, M., Ohno, S., Kawamoto, T., Satakeda, H., Akagawa, Y., Nakashima, K., Okimura, A., Ishida, H., Okamoto, T., Pan, H., Shen, M., Yan, W., and Kato, Y. Characterization of a cartilage-derived 66-kDa protein (RGD-CAP/beta ig-h3) that binds to collagen. Biochim Biophys Acta **1355,** 303, 1997.
37. Hecht, J.T., Montufar-Solis, D., Decker, G., Lawler, J., Daniels, K., and Duke, P.J. Retention of cartilage oligomeric matrix protein (COMP) and cell death in redifferentiated pseudoachondroplasiachondrocytes. Matrix Biol **17,** 625, 1998.
38. Rao, R.V., Peel, A., Logvinova, A., del Rio, G., and Hermel, E. Coupling endoplasmic reticulum stress to the cell death program: role of the ER chaperone GRP78. FEBS Lett **514,** 122, 2002.
39. Lu, Z., Doulabi, B.Z., Huang, C., Bank, R.A., and Helder, M.N. Collagen type II enhances chondrogenesis in adipose tissue-derived stem cells by affecting cell shape. Tissue Eng Part A **16,** 81, 2010.
40. Brekken, R.A., and Sage, E.H. SPARC, a matricellular protein: at the crossroads of cell-matrix communication. Matrix Biol **19,** 816, 2001.
41. Hecht, J.T., and Sage, E.H. Retention of the matricellular protein SPARC in the endoplasmic reticulum of chondrocytes from patients with pseudoachondroplasia. J Histochem Cytochem **54,** 269, 2006.
42. Woods, A., Wang, G., and Beier, F. Regulation of chondrocyte differentiation by the actin cytoskeleton and adhesive interactions. J Cell Physiol **213,** 1, 2007.
43. Wang, W., Xu, J., and Kirsch, T. Annexin-mediated Ca2+ influx regulates growth plate chondrocyte maturation and apoptosis. J Biol Chem **278,** 3762, 2003.
44. Kirsch, T. Annexins - their role in cartilage mineralization. Front Biosci **10,** 576, 2005.
45. Silver, I.A. Measurement of pH and ionic composition of pericellular sites. Philos Trans R Soc Lond B Biol Sci **271,** 261, 1975.
46. Spencer, C.A., Palmer, T.N., and Mason, R.M. Intermediary metabolism in the Swarm rat chondrosarcoma chondrocyte. Biochem J **265,** 911, 1990.
47. Otte, P. Basic cell metabolism of articular cartilage. Manometric studies. Z Rheumatol **50,** 304, 1991.
48. Semenza, G.L. Expression of hypoxia-inducible factor 1: mechanisms and consequences. Biochem Pharmacol **59,** 47, 2000.
49. Ruiz-Romero, C., Carreira, V., Rego, I., Remeseiro, S., López-Armada, M.J., and Blanco, F.J. Proteomic analysis of human osteoarthritic chondrocytes reveals protein changes in stress and glycolysis. Proteomics **8,** 495, 2008.
50. Wang, D.W., Fermor, B., Gimble, J.M., Awad, H.A., and Guilak, F. Influence of oxygen on the proliferation and metabolism of adipose derived adult stem cells. J Cell Physiol **204,** 184, 2005.
51. Pilgaard, L., Lund, P., Duroux, M., Fink, T., Ulrich-Vinther, M., Søballe, K., and Zachar V. Effect of oxygen concentration, culture format and donor variability on *in vitro* chondrogenesis of human adipose tissue-derived stem cells. Regen Med **4,** 539, 2009.

Address correspondence to:
Lei Cui, PhD, MD
Department of Plastic and Reconstructive Surgery
Shanghai 9th People's Hospital
Shanghai Jiao Tong University School of Medicine
639 Zhi Zao Ju Road
Shanghai 200011
People's Republic of China

E-mail: leicuimd@yahoo.cn

Received: April 5, 2013
Accepted: September 10, 2013
Online Publication Date: November 13, 2013